Electron-phonon interactions of nonequilibrium charge carriers in $YBa_2Cu_3O_{7-\delta}$ investigated by picosecond resonance Raman spectroscopy

I. Poberaj and D. Mihailovic
Jozef Stefan Institute, University of Ljubljana, Jamova 39, Ljubljana, Slovenia
(Received 22 April 1994)

The electron-phonon coupling of photoexcited carriers is investigated in $YBa_2Cu_3O_{7-\delta}$ (YBCO) with $\delta = 0.8$ and 0.1 by measuring nonequilibrium phonon occupation numbers n_{ph} on the ultrashort timescale with picosecond Stokes and anti-Stokes resonant Raman spectroscopy. In both insulating and metallic materials significant nonequilibrium n_{ph} are observed due to the interaction of carriers with lattice vibrations. Increasing the photoexcited carrier density to beyond $\sim 10^{19}$ cm^{-3} in $YBa_2Cu_3O_{6.2}$, an abrupt change of both the electron-phonon coupling and reflectivity is observed, as a consequence of a photoinduced insulator-to-metal (I-M) transition. Whereas n_{ph} of the apical O vibrations is found to increase with increasing excited carrier density with a change of slope at the I-M transition, n_{ph} for the planar 340 cm^{-1} vibration shows a marked decrease of coupling in the metallic state. The clear implication is that whereas the out-of-plane carrier interaction with apical O vibrations remains quite strong in both the insulating and metallic phases, the in-plane coupling is significantly reduced in the metallic phase of the material.

I. INTRODUCTION

The character of charge carriers in high-temperature oxide superconductors has been the subject of intense experimental and theoretical investigation ever since the discovery of superconductivity in these materials by Bednorz and Müller.[1] Both the electron-phonon interaction and carrier correlation effects are thought to be important in the superconducting materials, and new experimental results which give microscopic details of these interactions are in clear demand. The important questions that remain to be answered are whether carriers in these materials contain a significant phonon dressing, which lattice vibrations are of importance, and what changes take place with doping. Clearly of special interest are those lattice vibrations for which there is already some evidence that they may be part of a polaron,[2] for example, the A_g-symmetry c-axis apical O vibrations in YBCO and similarly structured materials. The importance of this particular vibration comes from its involvement in the c-axis charge transfer from the out-of-plane structure to the CuO_2 planes. Since this vibration modulates energy bands[3] near E_F with ω_{ph}, it is of direct relevance to superconductivity.

II. EXPERIMENTAL METHOD

In trying to answer some of these still unanswered fundamental questions we investigate the coupling of photoexcited (PE) carriers to different lattice vibrations by Raman spectroscopy. We report results as a function of PE carrier density in insulating $YBa_2Cu_3O_{6.2}$ as well as both chemically and photoinduced metallic $YBa_2Cu_3O_{7-\delta}$. We compare the n_{ph} of two optic phonons in YBCO of very different character: the 340 cm^{-1} Raman mode belonging to the O(2)/O(3) c-axis out-of-phase vibration (sometimes referred to as the plane-buckling vibration), and the 470 cm^{-1} mode belonging to the out-of-plane apical O(4) "charge transfer" vibration.[4] Carriers out of equilibrium which strongly scatter from or emit phonons can be thought to give an additional nonequilibrium contribution n_{neq} to the phonon occupation number,[5] such that the total phonon occupation is

$$n_{ph} = n_{eq} + n_{neq}, \tag{1}$$

where n_{eq} is the equilibrium phonon population given by the Bose-Einstein distribution function $n_{eq} = [\exp(\hbar\omega_{ph}/k_BT) - 1]^{-1}$, where ω_{ph} is the phonon frequency and T is the temperature. n_{ph} for each phonon is determined directly from the Stokes and anti-Stokes scattering intensities in Raman spectroscopy using $n_{ph} = (I_S/I_A - 1)^{-1}$. Although, strictly speaking, n_{ph} is defined by the fluctuation-dissipation theorem for equilibrium conditions only, we presently use n_{ph} as an *observable parameter*, bearing in mind that the distribution function may depart from Bose-Einstein statistics when $n_{neq} > 0$.

A. Excitation process

To excite a nonequilibrium population n_{neq}, we use intense ultrashort laser pulses. The sequence of events after photoexcitation by a laser pulse is reasonably well understood[6,7] in $YBa_2Cu_3O_{7-\delta}$. Optical absorption in z polarization (i.e., $\|$ c axis) at 2.33 eV in both insulating $YBa_2Cu_3O_6$ and metallic $YBa_2Cu_3O_{7-\delta}$ ($0 < \delta < 0.65$) proceeds via charge transfer (CT) between chain states and plane states. x or y excitation in $YBa_2Cu_3O_6$

0163-1829/94/50(9)/6426(5)/$06.00

results in an in-plane CT, while the x or y excitation ($\|$ a or b) in metallic $YBa_2Cu_3O_7$ is more complicated (but understood).[6] To some extent the choice of incident light polarization thus enables us to study the dynamics of excited carriers in different energy states. For carrier relaxation within a band, kinetic energy of the PE charge carriers is first distributed within themselves within a few hundred femtoseconds[8] and subsequently transferred to the lattice via scattering with phonons. These phonons then decay anharmonically to other phonons and disperse, eventually heating the whole crystal. In a Fermi glass, where the states are localized, relaxation towards equilibrium proceeds by activated hopping, the localized states being either self-trapped polarons[2] or defects. In both cases we expect to observe a nonequilibrium effect due to the photoexcited carriers, and all we require is that the laser pulse duration $\tau_L \sim \tau_c$, where τ_c is the carrier lifetime. Given that the phonon lifetimes do not vary significantly with doping,[9] any effects we observe will be due to changes in the e-p coupling.

B. Experimental details

Short laser pulses were generated with the aid of a Raman intensity-stabilized optical fiber pulse compressor[10] giving pulses of $\tau_L = 0.5$–3 ps. 100 ps pulses from a Quantronix mode-locked Nd:YAG laser and an Iskra extra low-loss (0.36 dB/km at 1.06 μm) optical fiber with high-efficiency 1200 lpm American Holographic gratings were used for this purpose. The frequency doubled output from the compressor gives a 100 MHz pulse train with an average power of 15 mW at 532 nm (2.33 eV). For cw excitation we have used 514.5 nm light from an Ar ion laser. Stokes and anti-Stokes spectra were recorded simultaneously using a Kaiser Optics holographic Super-Notch filter and an apodized central slit in the filter stage of a SPEX Triplemate monochromator. All the present experiments were performed on well characterized ($\rho(T), \chi(T)$, Raman) single crystals. The desired oxygen concentration was achieved by annealing the samples in Ar gas.

C. Nonequilibrium phonon counting

A nonequilibrium population of phonons $n_{\rm ph}$ is measurable during the overlap in time between the laser pulse and the nonequilibrium carrier population. The time dependence of the excess charge carrier concentration $n_c(t)$ is obtained by solving

$$\frac{dn_c(t)}{dt} = G(t) - \frac{n_c(t)}{\tau_c}, \tag{2}$$

where τ_c is the carrier lifetime and $G(t) = G_0/\tau_L\sqrt{2/\pi}\,\exp -[2(t-t_0)^2/(\tau_L^2)]$ is the rate at which carriers are photogenerated, assuming a Gaussian temporal pulse profile of width τ_L. The solution to (2) is given by

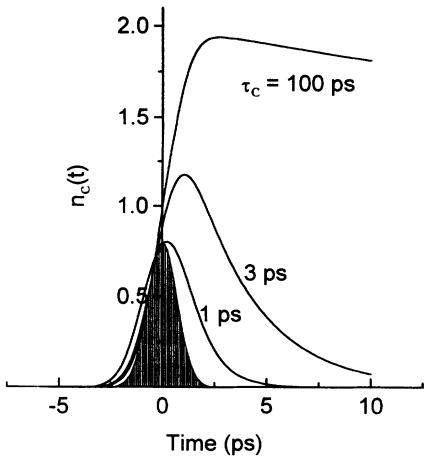

FIG. 1. Raman scattering occurs while the short laser pulse (shaded) overlaps with the nonequilibrium phonon population, shown here for three different carrier lifetimes, τ_c.

$$n_c(t) = \frac{G_0}{2}\exp\frac{-8(t-t_0)\tau_c + \tau_L^2}{8\tau_c^2} \times\left\{\mathrm{erf}\left[\sqrt{2}\left(\frac{(t-t_0)}{\tau_L} - \frac{\tau_L}{4\tau_c}\right)\right] + 1\right\} \tag{3}$$

and is plotted in Fig. 1 for three different values of τ_c and $\tau_L = 1$ ps. With peak fluences of 10^{16} photons/cm^{-2}, the PE carrier density in YBCO reachable in our experiments is in the range $\sim 10^{19}$–10^{21} cm^{-3}; i.e., metallic carrier densities are easily obtained.

III. RESULTS

The Raman spectra of $YBa_2Cu_3O_{7-\delta}$ using 1.5 ps and 100 ps laser excitation, both at 532 nm and identical average laser power, are shown in Fig. 2. Spectra in two scattering geometries are shown, such that the apical O(4) phonon at 470 cm^{-1} ($zz + zx$) and the Cu-O plane buckling phonon at 340 cm^{-1} ($xx + xz$) are both observed. We see that the anti-Stokes scattering intensity is significantly higher in the 1.5 ps Raman spectra than in the 100 ps Raman spectra indicating significant coupling to the PE carriers, but otherwise the spectra have no major additional features.

$n_{\rm ph}$ can have an offset due to slightly different resonance enhancements and/or reabsorption of the Stokes and anti-Stokes photons in the material. Since the resonance profiles and $\epsilon(\omega)$ are known[6] for YBCO, we have been able to account for these effects (including possible photoinduced changes). It turns out that these effects are small and do not significantly affect the present experiments. By measuring the I_S/I_A ratio with very low laser power density cw excitation at 514.5 nm and 100 ps laser excitation at 532 nm we confirm experimentally that the offset is negligible for *both* $YBa_2Cu_3O_{6.2}$ and $YBa_2Cu_3O_{6.9}$ near $\lambda_L = 532$ nm. Just as importantly with these cw and long-pulse measurements we also determine $n_{\rm ph}$ in the asymptotic limit of low photoexcitation density.

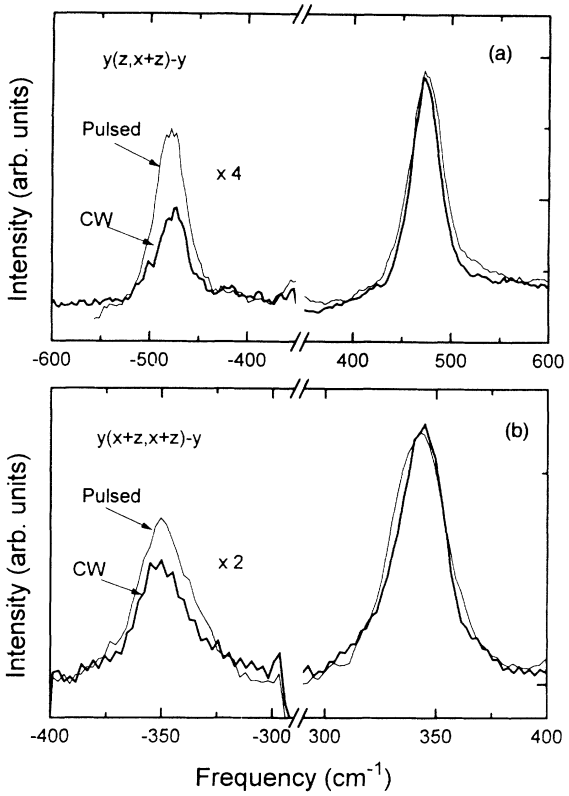

FIG. 2. Raman spectra of $YBa_2Cu_3O_{6.2}$ showing Stokes and anti-Stokes scattering (a) for the 470 cm^{-1} apical O(4) phonon and (b) for the plane buckling 340 cm^{-1} mode taken with 1.5 ps laser pulses (thin curve).

Changing the peak incident laser fluence we observe a number of nontrivial effects which are shown in Figs. 3 and 4. Importantly, from an experimental point of view, the data were taken in random order to avoid errors due to possible systematic drift of pulse width with time.

(1) In $YBa_2Cu_3O_{6.2}$ for electric field $E \parallel c$ [Fig. 3(a)], the apical O phonon at 470 cm^{-1} occupation number n_{470} first rapidly rises above the 300 K value of n_{eq}=0.1 and then changes slope at $\mathcal{F} \sim 2 \times 10^{12}$ photons/cm^2 whereupon it keeps increasing linearly. The discontinuity or knee at $\mathcal{F} \sim 2\times10^{12}$ photons/cm^2 corresponds to a PE carrier density of $\sim 10^{19}$ cm^{-3}. This is somewhat lower than where we expect the insulator-to-metal transition to occur (perhaps at a few $\times10^{20}$) and may be due to electronic phase separation.

(2) For $E \parallel a$, n_{340} consistently first rises from n_{eq}=0.24 at low flux density to a maximum of n_{ph}=0.35 at $\mathcal{F} \sim 1 \times 10^{12}$ photons/cm^2, then decreases at intermediate power, and finally increases again at high excitation powers [Fig. 3(b)]. The discontinuity appears at somewhat lower $\mathcal{F}$ for n_{340} than for n_{470}, because of the shorter absorption length at 2.33 eV for phonons with $E \parallel a$.

(3) In contrast to the experiment on insulating $YBa_2Cu_3O_{6.2}$ above, in chemically doped $YBa_2Cu_3O_{6.9}$ with $E \parallel c$, n_{500} for the apical O vibration (which is now shifted to 500 cm^{-1}) increases monotonically from n_{eq} = 0.1 [Fig. 3(c)] with a slope similar to that of n_{470} in the metallic phase possibly implying more than just a superficial equivalence between PE and chemical doping.

(4) Confirming the existence of an *I-M* transition, in Fig. 4 we show a significant nonlinear change in reflectivity, R as a function of PE intensity. As expected, the change is large initially and the change in R of ~10% is similar to the observed change in $\epsilon(\omega)$ with chemical doping at this energy.[6]

(5) We also note a small frequency shift of the phonons with increasing photoexcitation (Fig. 2). The slight, 4 cm^{-1} *increase* of the 470 cm^{-1} phonon and the small, 3 cm^{-1} *decrease* in frequency of the 340 cm^{-1} phonon is exactly what we would expect comparing the photoexcitation experiment to chemical doping.[4,11]

Repeating the measurements with 100 ps pulses at 532 nm of the same average power or a cw Ar laser excitation at 514.5 nm n_{ph} now increases only slightly because of laser heating, and in very good agreement with the calculated value of n_{ph} for laser heating (Fig. 3).

IV. DISCUSSION

A. Heating effects

The very different behavior of the three O phonons and comparison of 1.5 ps with 100 ps pulse and cw experiments immediately rule out simple lattice heating effects. We can quite accurately calculate the laser heating contribution to n_{ph} by calculating the surface temperature of the sample. This was done by adapting the solution of the thermal diffusion equation calculated by Bechtel[12] to the case of a train of 1.5 ps laser pulses absorbed on the sample surface, taking into account both inward and lateral thermal diffusion[13] as well as heat buildup. The results are drawn as solid lines in Fig. 3. As expected, laser heating can explain only the cw behavior and certainly not the unusual behavior of n_{ph} in Fig. 3.

The calculation of sample heating above assumes that the lattice as a whole absorbs all the heat. On the picosecond time scale the system is out of equilibrium, and so for the sake of argument, let us assume that the energy is transferred to only a few (say, $\eta \sim 5$) phonons rather than the lattice as a whole. The specific heat of the system would then be reduced by η/N, where N is the total number of phonons (N=39 in $YB_2Cu_3O_{7-\delta}$). This increases the sample temperature[12] by a factor of N/η and implies an increase in slope of n_{ph} vs incident photon flux in Fig. 3(a) of ~ 2.8, i.e., still not enough to explain the data. We can understand the data only if we assume a preferential interaction of the PE carriers with the apical O vibrations which takes place over a limited part of the Brillouin zone Δk. In other words, the interaction responsible for the effects we see appears to be semilocalized with range $r \sim 2\pi/\Delta k$. The appropriate description of YBCO would thus be that of a Fermi glass rather than a band semiconductor or metal.

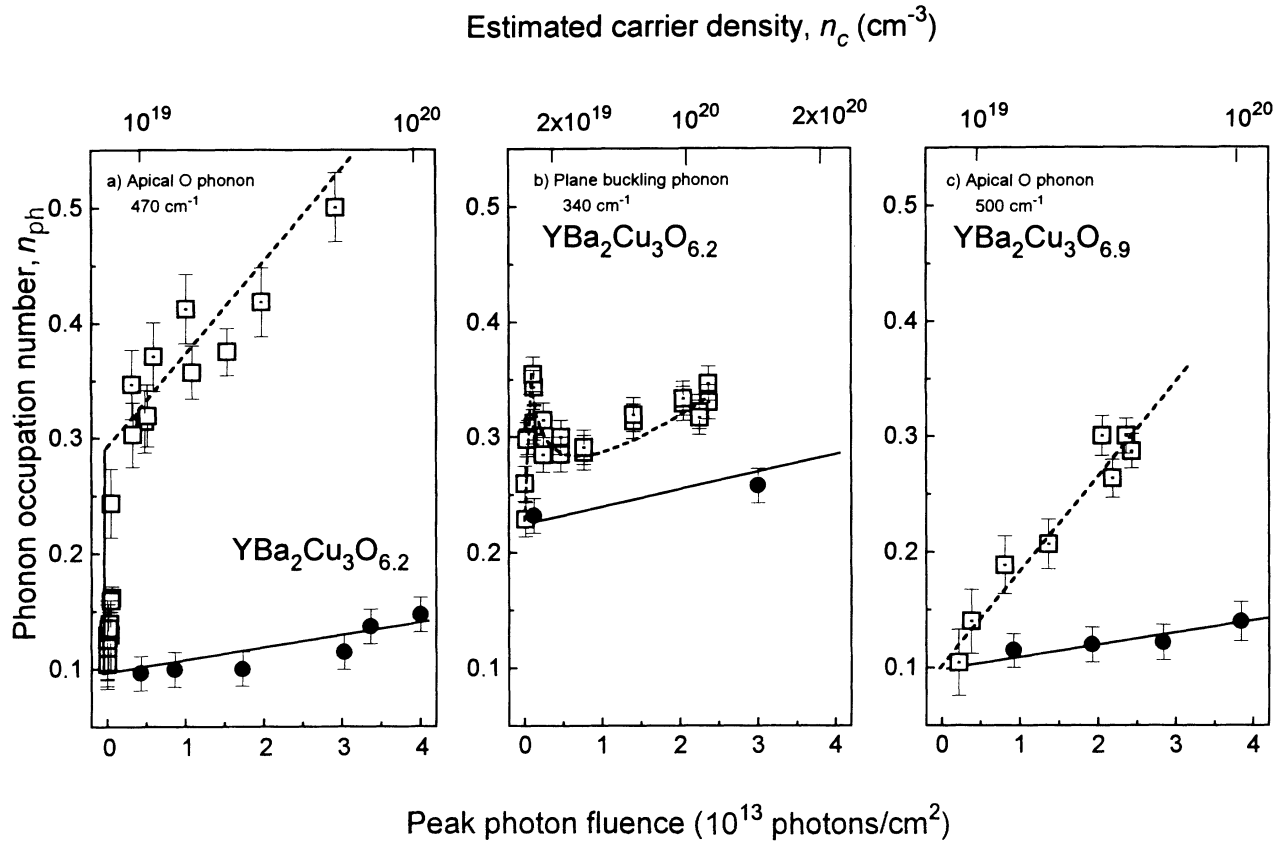

FIG. 3. Phonon occupation number $n_{\rm ph}$ as a function of peak incident photon fluence $\mathcal{F}$ for (a) the 470 cm^{-1} apical O mode in $YBa_2Cu_3O_{6.2}$, (b) the 340 cm^{-1} phonon also in $YBa_2Cu_3O_{6.2}$, and (c) for the 500 cm^{-1} apical O mode in $YBa_2Cu_3O_{6.9}$. All data in open squares are taken with 1.5 ps pulses. The estimated PE carrier density (assuming uniform density) is shown on the top axis. The solid lines show the calculated phonon occupation number at the sample temperature. Dashed lines are guides to the eye. For camparison, the solid circles are taken with 514.5 nm cw excitation, all with the same *average* laser power.

B. Electron-phonon coupling of nonequilibrium carriers

In $YBa_2Cu_3O_{6.2}$ photoexcitation along c (zz or zx Raman scattering geometry) results in a charge transfer of an electron from the CuO_2 planes to states of the Cu-O chains or dumbbells (depending on the extent of oxygenation), leaving behind a hole in the CuO_2 planes.[6,7] (Chemical doping is effectively the same: Chain O(1) atoms pull electrons from the CuO_2 planes leaving them doped with holes.) At $\delta \simeq 0.65$ there is a well-defined doping-induced I-M transition, which corresponds approximately to a plane carrier density of 10^{19}–10^{20} cm^{-3}. The discontinuity in n_{470} and n_{340} at $n_c \sim 10^{19}$ cm^{-3} ($\mathcal{F} \sim 2\times10^{12}$ photons/cm^2) is thus apparently related to a change in the electron-phonon coupling of the carriers on crossing the I-M transition. In the metallic phase we expect the charge carriers (especially holes) to delocalize and the carrier-carrier interaction to change. Hence a reduction in e-p coupling and $n_{\rm ph}$, especially for n_{340}, is understandable: Itinerant holes in the planes are not ex-

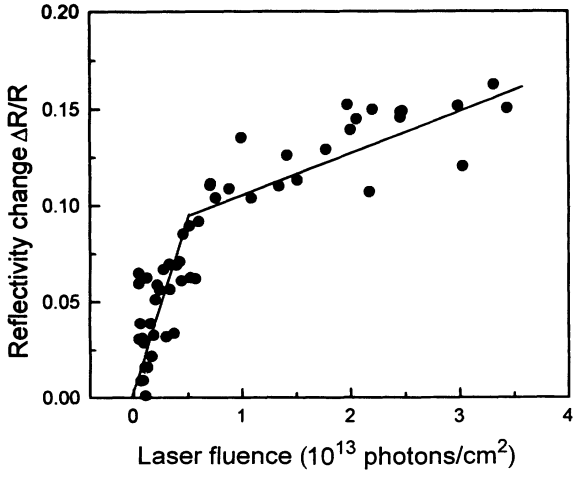

FIG. 4. Reflectivity change $\Delta R/R$ for unpolarized light at 2.33 eV incident on the crystal ac plane, as a function of incident photon fluence $\mathcal{F}$. The line is a guide to the eye. A break in $\Delta R/R$ is clearly visible at $\mathcal{F} \sim 2\times10^{12}$ photons/cm^2.

pected to give rise to strongly coupled polaronic states.[14] On the microscopic scale we can identify the large effect on the apical O phonon n_{ph} as fairly convincing evidence of strong *e-p* coupling of this out-of-plane A_g mode to PE carriers and suggests carriers localized *in the chains*, rather than CuO_2 planes.

On the other hand, photoexcitation along *a* (or *b*) at 2.33 eV gives rise to a charge transfer within the CuO_2 planes.[6] Judging by the increase in n_{340} above n_{eq} for $\mathcal{F} \sim 10^{12}$ photons/cm^2, i.e., in the insulating phase with low photoexcited carrier density, carriers are localized creating a distortion involving the plane-buckling 340 cm $^{-1}$ phonon. As the holes become itinerant above $\mathcal{F} \sim 10^{12}$ photons/cm^2, the plane-buckling distortion is apparently rapidly reduced, reducing n_{ph}. The data thus suggest that in-plane carriers are significantly less coupled to phonons than chain carriers.

The scenario of the simultaneous presence of two types of carriers (chain polarons and more itinerant planar holes) can straightforwardly explain the Drude peak and the midinfrared feature observed in $\sigma(\omega)$, especially the *a-b* anisotropy observed in the mid-IR region.[15] We can thus assign the mainly temperature-independent mid-IR band (which is polarized along the Cu-O chains in YBCO) to the chain polarons, and the Drude-like strongly temperature-dependent peak to the planar carriers, which behave in a more bandlike fashion. The two-carrier scenario also opens some interesting possibilities for superconductivity, where (bi)polarons take the place of phonons in a BCS-like scenario. Two in-plane holes would thus be paired by a *c*-axis charge transfer, which could in turn be associated with polaronic hopping outside the planes. The correlation between T_c and the polarizability of the charge reservoirs (which is superficially related to the size of the unit cell) could thus be explained.

V. CONCLUSION

In conclusion, by using selective in-plane ($\| a,b$) or out-of-plane ($\| c$) photoexcitation in YBCO and measuring individually the nonequilibrium properties of different O vibrations with short-pulse Raman spectroscopy, we can observe significant nonequilibrium populations of apical O(4) and plane-buckling phonons, which are believed to be due to strong *e-p* coupling consistent with the formation of PE lattice polarons. By increasing the PE carrier density above the Mott limit, an *I-M* transition is indicated both by a change in sample reflectivity and a qualitative change in the *e-p* coupling. The existence of the PE metallic state in YBCO directly confirms the transient photoconductivity experiments of Yu and Heeger.[16] The onset of the metallic phase and hole itinerancy is coincident with the significant reduction of a B_{1g} plane-buckling 340 cm^{-1} mode distortion, while strongly coupled charge carriers involving A_g apical O phonons most likely in Cu-O chains are apparently present in both the insulating and metallic phases of YBCO.

ACKNOWLEDGMENTS

We wish to acknowledge the donation of samples by P. Tholence, H. Noel, and G. Collin as well as valuable comments from J. Ranninger, M. Copic, P. Gosar, and J.F. Ryan. This work has been supported in part by CEC Grant No. CI1 0568-C.

[1] J.G. Bednorz and K.A. Müller, Z. Phys. B **64**, 189 (1986).
[2] D. Mihailovic *et al.*, Phys. Rev. B **44**, 237 (1991), and references therein; C. Taliani *et al.*, Solid State Commun. **65**, 487 (1988); K.A. Müller, Z. Phys. B **80**, 193 (1990).
[3] O.K. Andersen, Physica C **185-189**, 187 (1991).
[4] C. Thomsen and M. Cardona, in *Physical Properties of High Temperature Superconductors I*, edited by D.M. Ginsberg (World Scientific, Singapore, 1989).
[5] J. Ranninger and U. Thibblin, Phys. Rev. B **45**, 7730 (1992).
[6] E.T. Heyen, J. Kircher, and M. Cardona, Phys. Rev. B **45**, 3037 (1992); E.T. Heyen *et al.*, Phys. Rev. Lett. **65**, 3048 (1990); O.K. Misochko, E.Ya. Sherman, and V.B. Timofeev, Physica C **185**, 1025 (1991).
[7] G. Yu *et al.*, Phys. Rev. B **48**, 7545 (1993).
[8] S.G. Han *et al.*, Phys. Rev. Lett. **65**, 2708 (1990).
[9] In spite of extensive search, no correlation has ever been found between any phonon linewidths and doping. A discussion of the intrinsic lifetimes is given in D. Mihailovic *et al.*, Phys. Rev. B **47**, 8910 (1993).
[10] J.P. Heritage, A.M. Weiner, R.J. Hawkins, and O.E. Martinez, Opt. Commun. **67**, 367 (1988).
[11] Only systems where direct doping of the Cu-O planes takes place without structural changes can be compared. See for example T. Mertelj *et al.*, Phys. Rev. B **47**, 12104 (1993).
[12] J.H. Bechtel, J. Appl. Phys. **46**, 1585 (1975), Eq. (4.2).
[13] The values of constants used for YBCO were: The absorption length, $l = 0.06$ μm at 2.33 eV, the thermal diffusivity, $\kappa = K/\rho c$, where $K = 5$ Wm^{-1}K^{-1} is the thermal conductivity, $\rho = 6.38$ g cm^{-3} the density, and $c = 300$ JK^{-1}mol^{-1} is the specific heat capacity.
[14] J. Ranninger, Solid State Commun. **85**, 929 (1993).
[15] L.D. Rotter *et al.*, Phys. Rev. Lett. **67**, 2741 (1991).
[16] G.Yu *et al.*, Phys. Rev. Lett. **67**, 2581 (1991).